CHEMISTRY
A EUROPEAN JOURNAL

DOI: 10.1002/chem.200601870

The Ball-Shaped Heteropolytungstates $[\{Sn(CH_3)_2(H_2O)\}_{24}\{Sn(CH_3)_2\}_{12}(A\text{-}XW_9O_{34})_{12}]^{36-}$ (X = P, As): Stability, Redox and Electrocatalytic Properties in Aqueous Media

Bineta Keita,[a] Pedro de Oliveira,[a] Louis Nadjo,*[a] and Ulrich Kortz[b]

Abstract: The electrochemical behavior of the ball-shaped heteropolytungstates $[\{Sn(CH_3)_2(H_2O)\}_{24}\{Sn(CH_3)_2\}_{12}(A\text{-}XW_9O_{34})_{12}]^{36-}$ (X = P, **1**; As, **2**) was examined in aqueous electrolytes by redissolution of their respective mixed cesium–sodium salts $Cs_{14}Na_{22}[\{Sn(CH_3)_2(H_2O)\}_{24}\{Sn(CH_3)_2\}_{12}(A\text{-}PW_9O_{34})_{12}]\cdot 149\,H_2O$ (**Cs_{14}-1**) and $Cs_{14}Na_{22}[\{Sn(CH_3)_2(H_2O)\}_{24}\{Sn(CH_3)_2\}_{12}(A\text{-}AsW_9O_{34})_{12}]\cdot 149\,H_2O$ (**Cs_{14}-2**). In the studied media, **Cs_{14}-2** is readily soluble in contrast to the significantly less soluble **Cs_{14}-1**. The solubility of **Cs_{14}-1** is increased by the presence of Li^+ ions in solution. Gel filtration studies with **1** and **2** rule out a decay of the dodecameric spherical assemblies to Keggin-based monomers on the timescale of the experiment. By UV/Vis spectroscopy and cyclic voltammetry, **2** was found to be significantly less stable than **1** and both polyanions also show rather different decomposition pathways. Polyanion **1** collapses first into Keggin-type monomers which might contain the trilacunary $[A\text{-}\alpha\text{-}PW_9O_{34}]^{9-}$. The final monomeric species obtained from **1** appears to be very similar to $[PW_{11}O_{39}]^{7-}$, which is the final transformation product of $[A\text{-}\alpha\text{-}PW_9O_{34}]^{9-}$ in the same media. In contrast, **2** does not seem to follow an analogous transformation pathway as that of the trilacunary $[A\text{-}\alpha\text{-}AsW_9O_{34}]^{9-}$. Importantly, stabilization of **1** is observed in chloride media. The fairly long-term stability of **1** in 1 M LiCl, pH 3, has allowed for its electrochemical study to be carried out. The solid-state cyclic voltammogram of **1** entrapped in a carbon paste electrode shows the same characteristics as **1** dissolved in chloride solutions, thus supporting the conclusion that the polyanion is stable in these environments. Controlled potential coulometry on **1** indicates that the number of electrons consumed in the first wave is larger than twenty. To our knowledge, **1** constitutes the first example of a molecule that can take up such a large number of electrons resulting in a chemically reversible W-wave. These properties show promise for future fundamental and applied studies. Polyanion **1** is also efficient in the electrocatalytic reduction of NO_x, including nitrate. Finally, a remarkable interaction was found between **1** and NO, a highly promising feature for biomimetic applications.

Keywords: cyclic voltammetry · electrocatalysis · electrochemistry · nitrogen oxides · polyoxometalates

Introduction

The class of polyoxometalates (POMs) and in particular their transition-metal-substituted derivatives continue to attract much attention, owing to their putative and realized applications in heterogeneous/homogeneous oxidation catalysis, electrocatalysis, medicine, materials science, photochemistry, analytical chemistry, and magnetochemistry.[1–7] In addition, the shape, size, composition, and symmetry of discrete, molecular POMs constitute highly attractive features. The mechanism of formation of POMs remains poorly understood and commonly described as self-assembly. Rational synthesis of fundamentally novel molecular POM architectures remains a major challenge, although the use of lacunary precursors often allows us to predict at least building blocks of the resulting POM structure. Giant POMs have attracted special attention, as they represent the largest and heaviest inorganic molecules ever made combined with structural beauty. For example, the isopolyanion $[Mo_{36}O_{112}(H_2O)_{18}]^{8-}$[8] and the heteropolyanions $[As_4W_{40}O_{140}]^{28-}$[9] and $[H_7P_8W_{48}O_{148}]^{33-}$[10,11] were the largest POMs for a long time.

[a] Dr. B. Keita, Dr. P. de Oliveira, Prof. L. Nadjo
Laboratoire de Chimie Physique, UMR 8000, CNRS
Equipe d'Electrochimie et Photoélectrochimie
Université Paris-Sud, Bâtiment 420
91405 Orsay Cedex (France)
Fax: (+33) 169-154-328
E-mail: nadjo@lcp.u-psud.fr

[b] Prof. U. Kortz
Jacobs University Bremen
School of Engineering and Science
P.O. Box 750 561, 28725 Bremen (Germany)

However, in recent years the number of structurally well-characterized gigantic POM species has grown rather fast. Besides the remarkable series of gigantic mixed-valence polyoxomolybdate rings and spheres reported by the group of Müller,[12,13] Pope and co-workers reported on a polytungstate with 148 tungsten atoms, $[As_{12}Ce_{16}(H_2O)_{36}W_{148}O524]^{76-}$.[14] Sécheresse et al. described several large polyanion assemblies containing the cationic oxo–thio linker $[Mo_2O_2S_2(OH_2)_6]^{2+}$.[15] One of us (U.K.) also reported several large-sized POMs, including a tungstoarsenate(III) with 65 tungsten atoms, prepared by self-condensation of the dilacunary precursor $[As_2W_{19}O_{67}(H_2O)]^{14-}$;[16] large tungstophosphates based on titanium(IV);[17,18] and recently the ball-shaped heteropolytungstates **1** and **2**.[19] In favorable cases, such large-sized structures might constitute interesting electron reservoirs and/or sinks. As a consequence, such possibilities deserve to be investigated through electrochemical characterization.

Here we report on the electrochemical and electrocatalytic behavior of **1** and **2** either dissolved in aqueous solutions or incorporated in a carbon paste. For this purpose, the stability of **1** and **2** in aqueous electrolytes has been studied and the decomposition pathways have been investigated, in order to detect experimental conditions suitable for the electrochemical characterization of these complexes.

Experimental Section

Synthesis: The mixed cesium-sodium salts of **1** and **2**, $Cs_{14}Na_{22}[\{Sn(CH_3)_2(H_2O)\}_{24}\{Sn(CH_3)_2\}_{12}(A\text{-}PW_9O_{34})_{12}]\cdot 149\,H_2O$ (**Cs_{14}-1**) and $Cs_{14}Na_{22}[\{Sn(CH_3)_2(H_2O)\}_{24}\{Sn(CH_3)_2\}_{12}(A\text{-}AsW_9O_{34})_{12}]\cdot 149\,H_2O$ (**Cs_{14}-2**), were prepared as previously described by us.[19] $[A\text{-}PW_9O_{34}]^{9-}$,[20] $[PW_{11}O_{39}]^{7-}$[21] and $[P_2W_{15}Mo_2VO_{62}]^{8-}$[7,22] were prepared by literature methods. All other reagents were used as purchased without further purification.

UV/Vis spectroscopy: Pure water was used throughout. It was obtained by passing it through a RiOs 8 unit followed by a Millipore-Q Academic purification set. All reagents were of high-purity grade and were used as purchased without further purification. The UV/Vis spectra were recorded on a Perkin-Elmer Lambda 19 spectrophotometer on solutions of **1** and **2** as concentrated as possible (vide infra for explanations). Matched 1.000 cm optical path quartz cuvettes were used. The compositions of the various media used were as follows: pure water; 1 M HCl, pH 0; 0.5 M H_2SO_4, pH 0.33; 1 M LiCl/HCl, pH 2, 3 and 4; 0.9 M LiCl/HCl, pH 1; 0.5 M Li_2SO_4/H_2SO_4, pH 3; 1 M CH_3CO_2Li/CH_2ClCO_2H, pH 3; 1 M CH_3CO_2Li/CH_3CO_2H, pH 4 and 5; 0.5 M Li_2SO_4/Tris, pH 7.

Gel filtration chromatography: A 40 cm × 1 cm^2 Sephadex G-50 (fine) column was used, which allows the separation of species the molecular masses of which fall in the range 500 to 10000 $gmol^{-1}$. Samples (1 mL of either 2×10^{-5} M of **1** or 5×10^{-4} M of **2**) were eluted at a rate of 1 $mL\,min^{-1}$. The elution buffers were 1 M LiCl, pH 3, in the case of **1** and pure water in the case of **2**. Each sample contained also 1×10^{-3} M of the blue Wells–Dawson POM $[P_2W_{15}Mo_2VO_{62}]^{8-}$ ($Mo_2VP_2W_{15}$), the molecular mass (MW 4055 $gmol^{-1}$) of which falls in the separation range of Sephadex G-50, allowing it to be used as a molecular mass standard to facilitate the visual inspection of the elution due to its color. Fractions (approximately 2 mL) were collected and analyzed by UV/Vis–NIR spectrophotometry with a Perkin-Elmer Lambda 19 spectrophotometer, which allowed to monitor the elution of the different species, each having its characteristic spectrum with strong absorption bands in the UV range ($Mo_2VP_2W_{15}$ being blue, has an absorption band at 600 nm, that is, in the visible range of the spectrum).

Electrochemical experiments: The solutions were deaerated thoroughly for at least 30 min with pure argon and kept under a positive pressure of this gas during the experiments.

NO was introduced in an oxygen-free electrochemical cell through a catheter connected to a sealed purging system previously filled with argon that excluded oxygen and allowed contaminants such as NO_x to be scavenged in 9 M KOH. NO was bubbled through the electrolyte in the electrochemical cell for 30 min, resulting in a NO-saturated solution (1 to 2 mM). The electrochemical cell was checked for leaks in the following way: solutions saturated with NO were kept for several hours and used for electrocatalytic reduction of this substrate; after removing NO by bubbling pure argon, no electroactivity of NO or a related species could be detected in the potential range from + 0.8 V to −0.8 V at pH 0.33.

The POM **Cs_{14}-1** was dissolved slowly in 1 M LiCl, pH 3.00. The dissolution process was sped up by bubbling argon through a freshly prepared solution for 15 minutes prior to the electrochemical experiment.

The source, mounting, and polishing of the glassy carbon (GC, Tokai, Japan) electrodes has been described previously.[23] The glassy carbon samples had a diameter of 3 mm. The electrochemical set-up was an EG & G 273 A driven by a PC with the M270 software. Potentials are quoted against a saturated calomel electrode (SCE). The counter electrode was a platinum gauze of large surface area.

Carbon-paste electrodes were prepared as previously described.[24] Typically, the carbon paste was obtained by thoroughly hand-mixing mineral oil (Aldrich) with 100 mg of Vulcan XC-72 and 6 mg of **Cs_{14}-1**. A portion of the paste was packed into a glass tube and the inner surface of this paste cylinder was pressed against a copper wire. The electrode surface was smoothened with a soft surface. All experiments were performed at room temperature.

Results and Discussion

Figure 1 shows a combined polyhedral/ball-and-stick representation of **1** and **2**, highlighting the dodecameric nature of these polyanions.

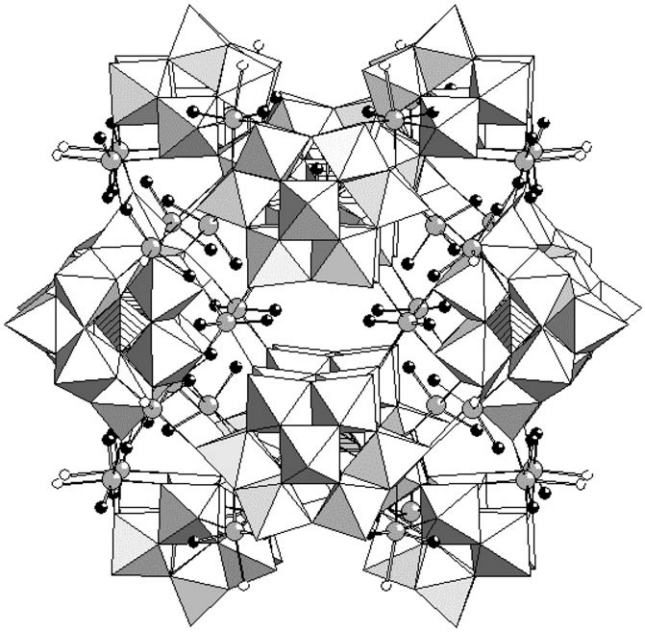

Figure 1. Combined polyhedral/ball-and-stick representation of **1** and **2**. The WO_6 octahedra are gray and the XO_4 tetrahedra (X = P, As) are hatched. The atoms are tin (grey spheres), oxygen (white spheres) and carbon (black spheres). No hydrogens shown for clarity.

Solubility of $Cs_{14}Na_{22}[\{Sn(CH_3)_2(H_2O)\}_{24}\{Sn(CH_3)_2\}_{12}(A\text{-}XW_9O_{34})_{12}]\cdot 149H_2O$ (X = P, Cs_{14}-1; As, Cs_{14}-2) and stability of $[\{Sn(CH_3)_2(H_2O)\}_{24}\{Sn(CH_3)_2\}_{12}(A\text{-}XW_9O_{34})_{12}]^{36-}$ (X = P, 1; As, 2): Solubility and stability tests were carried out in the various aqueous solutions mentioned in the Experimental Section, including pure water (Milli Q). **Cs_{14}-1** and **Cs_{14}-2** show very different dissolution behavior. By and large, **Cs_{14}-2** easily dissolved in all these media, whereas **Cs_{14}-1** required longer times for solutions to be obtained, and for some media concentrations as low as 2×10^{-5} M could not be prepared, even with stirring. This effect was particularly pronounced in pure water (Milli Q). The solubility of **Cs_{14}-1** increased significantly when an electrolyte containing Li^+ ions was present in the solution. For example, in NaCl media, **Cs_{14}-1** is very sparingly soluble at pH > 2 and this phenomenon increases with increasing the pH. The solubility can be increased upon replacing NaCl by LiCl. Analogously, a favorable presence of Li^+ ions was previously observed for the dissolution of the wheel-shaped tungstophosphate $[H_7P_8W_{48}O_{184}]^{33-}$.[25] Furthermore the dissolution of **Cs_{14}-1** and **Cs_{14}-2** in unbuffered LiCl media is accompanied by an important proton consumption. For instance, preparation of a 2×10^{-5} M solution of **1** in 1 M LiCl + HCl (pH 2.91) drives the final pH to 3.08, thus corresponding roughly to 20 H^+ consumed by each polyanion molecule. The pH increases with the polyanion concentration, resulting in a larger and larger ΔpH. In this respect, **2** follows the same trend as **1**. As a consequence, based on these observations it is necessary to measure the final pH when working with **1** and **2** in such media. Such remarks are especially important for the electrochemistry of **1** in these media, because POM electron-transfer reactions are accompanied by acid–base equilibria. Proton uptake has also been observed to accompany the dissolution of other large phosphotungstates, such as the wheel-shaped $[H_7P_8W_{48}O_{184}]^{33-}$ in unbuffered media.[25,26] Evidently, the pH of concentrated media with high buffer capacity was not affected by the presence of **1** or **2** at concentrations of around 4×10^{-5} M. For example, this was the case for 1 M CH_3CO_2Li/CH_2ClCO_2H, pH 3; 1 M CH_3CO_2Li/CH_3CO_2H, pH 4; and 0.9 M LiCl/HCl, pH 1. On the other hand, in 0.5 M Li_2SO_4/H_2SO_4, pH 3, there was a small effect for **1** ($\Delta pH \leq 0.04$), as expected for a solution with a medium buffer capacity due to HSO_4^-.

Long stirring times are required to obtain concentrations of **1** useful for standard electrochemical studies. As a result, the question arises for **1** (and also for **2**) if the polyanion maintains its solid-state structure in solution. To investigate this, the stability of **1** and **2** was assessed by UV/Vis spectrophotometry. The entire absorption spectrum and, in particular, the band at 240 nm, were monitored as a function of time. Upon the assumption that a very fast decomposition does not occur during dissolution prior to running the spectra, **1** was found to be fairly stable in pH 2–4 media. Interestingly, **2** turned out to be less stable than **1**. However, even for **1**, chloride media are necessary to enhance its stability. We also examined the possibility that the dodecameric **1** and **2** might decompose with time resulting in smaller POM fragments.

Therefore, we carried out gel filtration chromatography experiments on solutions of **1** and **2** in order to estimate their relative molecular sizes, using experimental conditions similar to the ones previously reported.[27] In this separation method, larger molecules are eluted first and smaller ones afterwards. Sephadex G-50 was used, which allows the separation of species the molecular masses of which fall in the range 500 to 10000 $gmol^{-1}$. The blue Wells-Dawson derivative $[P_2W_{15}Mo_2VO_{62}]^{8-}$ (**$Mo_2VP_2W_{15}$**; MW 4055 $gmol^{-1}$) was employed as a molecular mass standard. This blue species was the one to elute last from the Sephadex G-50 gel filtration column, irrespective of the ball-shaped heteropolytungstate present in the sample loaded into the column. Both **1** and **2**, having molecular masses > 30000 $gmol^{-1}$, should elute in the void volume, provided they do not decompose into smaller fragments with MW < 10000 $gmol^{-1}$. Indeed, **1** and **2** were detected in the very early fractions eluted from the column, and came out well before **$Mo_2VP_2W_{15}$**. This confirms that their molecular masses are larger than the upper separation limit of Sephadex G-50 (10000 $gmol^{-1}$). No species were detected eluting after **$Mo_2VP_2W_{15}$** on the timescale of the experiment (no more than 3 h), which rules out an eventual decay of either **1** or **2** to monomeric derivatives, the molecular masses of which would be around 2000–3000 $gmol^{-1}$ and which would have been found in fractions collected after the **$Mo_2VP_2W_{15}$** ones. Finally, it can be concluded, at the very least, that the decompositions of **1** and **2**, if any during the timescale of gel filtration experiments, must give tetrameric or higher oligomers. However, a complementary technique is needed to refine this conclusion. Cyclic voltammetry (CV) studies of **1** and **2** should fill this purpose and shed more light on electron uptake and release behaviors of these compounds in solution.

Cyclic voltammetry (CV) characterization: The results in the preceding section indicated roughly that **1** and **2** should be studied in more detail in pH 2–4 media. Several issues will be sequentially studied in the present section. Firstly, studies at pH 4 will monitor the CV behavior of **1** and **2** and try to assess their stability or decomposition pathways. Secondly, the composition of the various electrolytes will be shown to influence the stability of **1** and **2**. Finally, the results of these two sub-sections will be important for selecting conditions in which **1** is stable long enough for its detailed characterization by CV, described in the third sub-section.

Studies at pH 4 (1 M $CH_3COOLi + CH_3COOH$): Due to its higher stability, compound **1** was selected first for a detailed study. No redox activity was detected for the dimethyltin moities in this polyanion. This is in full agreement with the observations of Chorghade and Pope on Keggin- and Wells–Dawson-type tungstostannates,[28] and more recently by our group on $[\{Sn(CH_3)_2\}_4(H_2P_4W_{24}O_{92})_2]^{28-}$.[29] As a consequence, our focus was directed to the W-waves. Figure 2A shows a superposition of the CVs obtained in a pH 4 acetate medium for 2×10^{-5} M **1** and 2×10^{-4} M $[A\text{-}PW_9O_{34}]^{9-}$, the

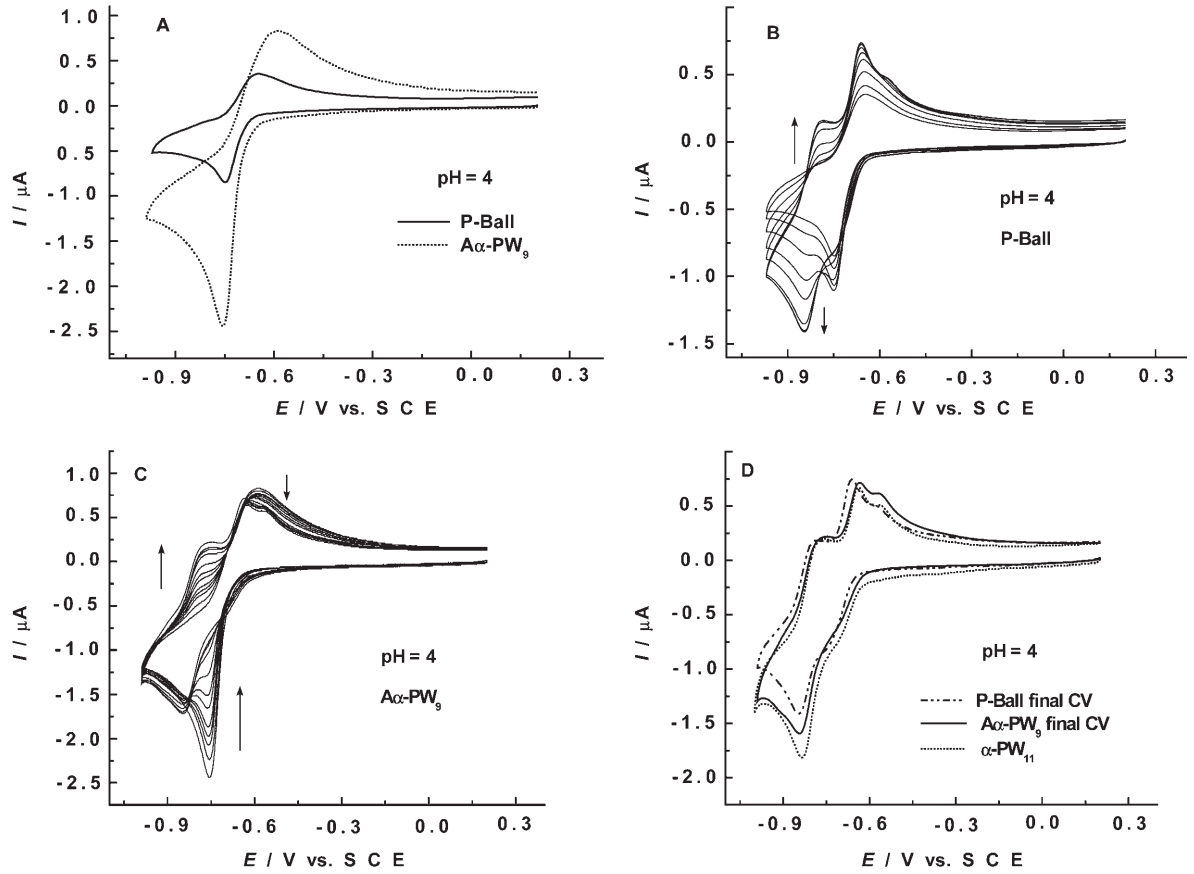

Figure 2. Cyclic voltammograms (CVs) of 2×10^{-5} M **1**, 2×10^{-4} M $[A\text{-}\alpha\text{-}PW_9O_{34}]^{9-}$ and 2×10^{-4} M $[PW_{11}O_{39}]^{7-}$ in a pH 4 medium (1 M CH_3CO_2Li/CH_3CO_2H). The scan rate was 10 mV s^{-1}, the working electrode was glassy carbon and the reference electrode was SCE. A) Superposition of the "initial" CVs of **1** and $[A\text{-}\alpha\text{-}PW_9O_{34}]^{9-}$. B) Evolution of the CV of **1** with time. C) Evolution of the CV of $[A\text{-}\alpha\text{-}PW_9O_{34}]^{9-}$ with time. D) Superposition of the "final" CVs of **1** and $[A\text{-}\alpha\text{-}PW_9O_{34}]^{9-}$. The CV of $[PW_{11}O_{39}]^{7-}$ is shown for comparison.

latter representing one of the possible decompostion products of the former. In addition, pH 4 guarantees a stability domain sufficient for its electrochemical study to be carried out for the trilacunary phosphotungstate precursor. The curves represent the first CV run or the first of several runs with the polyanions, on a timescale for which no modification on the curves could be detected. Figure 2A calls for several remarks. The two CVs have the same general shape. Such close resemblance of the W-wave shapes between a substituted polyanion and its lacunary precursor is not uncommon and has been pointed out several times previously.[7] However, the formal potentials E^0, calculated as the average between the cathodic and anodic peak potentials, are −0.700 V for **1** and −0.667 V for $[A\text{-}PW_9O_{34}]^{9-}$, and the anodic to cathodic peak potential differences (ΔE_p) are 0.096 V for **1** and 0.162 V for the POM precursor. Electronic influences of the dimethyltin substituents in **1** compared to $[A\text{-}PW_9O_{34}]^{9-}$ are reflected by the relative values of the formal potentials and the ΔE_p values. Finally, the peak current intensities (0.798 μA for **1** and 2.10 μA for the precursor) are strikingly different, which suggests the integrity of **1**. Its eventual decomposition into monomeric fragments should have resulted in roughly the same current as for $[A\text{-}PW_9O_{34}]^{9-}$. The peak current intensities should be governed by the individual diffusion coefficients of the polyanions and by the number of electrons consumed at each wave. It is known that the reduction of $[A\text{-}PW_9O_{34}]^{9-}$ is a four-electron process.[21] However, both **1** and $[A\text{-}PW_9O_{34}]^{9-}$ were found to undergo slow transformations in acetate pH 4 medium and therefore a detailed CV study at these conditions was not possible. It is worth noting that only the first characteristic wave of $[A\text{-}PW_9O_{34}]^{9-}$ is considered here, whereas a second, large-current, chemically irreversible wave close to the solvent discharge limit is not of relevance for this study.

In pH 4 medium and in the presence of Li^+ ions, the evolution of **1** and **2** was found to follow intermediate speed kinetics and could therefore be easily studied by electrochemistry. Figure 2B and 2C show the evolution of the CVs of **1** and $[A\text{-}PW_9O_{34}]^{9-}$, respectively, as a function of time. Focusing on the transformations of the trilacunary POM, Figure 2C shows its initial cyclic voltammogram that is mainly composed of a single, chemically reversible four-electron wave. A clearly detected transformation sets in rapidly and is represented by a two-wave system, as shown in selected cyclic voltammograms in Figure 2C. After roughly 6 h, the cyclic voltammogram stabilizes. We believe that [α-

$PW_{11}O_{39}]^{7-}$ is the final transformation product of [*A*-$PW_9O_{34}]^{9-}$ in our experimental conditions, based on studies with the three trilacunary Keggin isomers K_9[*A*-α-PW_9O_{34}], K_9[*A*-β-PW_9O_{34}] and K_9[*B*-α-PW_9O_{34}].[30] A comparison between the final CVs of [*A*-α-$PW_9O_{34}]^{9-}$ and that of an authentic sample of [α-$PW_{11}O_{39}]^{7-}$ confirms our hypothesis. We also verified that $[PW_{11}O_{39}]^{7-}$ is indeed stable in this pH 4 medium.

Figure 2B shows that the reversible wave of **1** also undergoes a progressive transformation into a two-wave system. However, the transformation processes of **1** and [*A*-α-$PW_9O_{34}]^{9-}$ are different: 1) the transformation of [*A*-α-$PW_9O_{34}]^{9-}$ is simple, resulting in the progressive disappearance of the four-electron wave, which is replaced by two two-electron waves attributed to [α-$PW_{11}O_{39}]^{7-}$; 2) the decomposition of **1** is more intricate: first, the peak current of the initial wave increases with the concomitant appearance of a second wave. The peak current of the first wave keeps increasing during the first hour of the experiment, then decreases and stabilizes after roughly 5 h. The peak current intensity of the second wave keeps increasing progressively during this entire process and finally stabilizes too. These observations can be easily rationalized by considering that the dodecameric **1** decomposes into monomeric entities. In this case, two processes co-exist that have opposite effects on the current intensity: 1) the decomposition into monomeric POM units should increase the current as it must be anticipated that these small entities have larger diffusion coefficients than the very large **1**; 2) the transformation of the unique initial wave of these monomers into a two-wave system should decrease the observed current as shown for [*A*-α-$PW_9O_{34}]^{9-}$ in Figure 2C. It is likely that **1** decomposes first resulting in fragments closely related to [*A*-α-$PW_9O_{34}]^{9-}$, which then follow a transformation pathway analogous to that of [*A*-α-$PW_9O_{34}]^{9-}$. Confirmation of this analogy appears in Figure 2D, which shows in superposition the final voltammetric patterns obtained from **1** and [*A*-α-$PW_9O_{34}]^{9-}$ and the voltammogram of an authentic sample of $[PW_{11}O_{39}]^{7-}$ in the same medium. It is worth noting that the current intensity of the CV associated with the transformation of **1** is practically the same as that of the analytical concentration of [*A*-α-$PW_9O_{34}]^{9-}$, thus suggesting a decomposition of the former polyanion into monomers. Scrutiny of the voltammograms in Figure 2D suggests, however, that these monomers might contain dimethyltin fragments, because the redox characteristics are not exactly the same as those of $[PW_{11}O_{39}]^{7-}$. This difference in redox characteristics suggests that monomeric species of the type $[\{Sn(CH_3)_2(H_2O)_2\}_xPW_9O_{34}]^{(9-2x)-}$ ($x=1$–3) could be present.

In Figure 3A one of the very first CVs of **2** is compared with that of **1** in pH 4 acetate medium and run on a timescale at which **1** has not yet initiated the transformation process described above. It should be mentioned that **2** is reduced at a slightly more positive potential than **1**, in agreement with the electrochemistry of most POMs with As and P hetero atoms.[7] Figure 3B shows a superposition of the CVs obtained in a pH 4 acetate medium for 2×10^{-5} M **2** and 2×10^{-4} M [*A*-α-$AsW_9O_{34}]^{9-}$ due to the dodecameric nature of the former POM. These CVs were run as soon as possible after dissolution of the respective materials. There are differences compared to Figure 2A, which we ascribe to the different solution behaviors of **1**, **2**, and their respective lacunary precursors [*A*-α-$XW_9O_{34}]^{9-}$ (X = P, As). Figure 3C and 3D, respectively, show two types of voltammetric patterns associated with the transformation of **2** and [*A*-α-$AsW_9O_{34}]^{9-}$ as a function of time. Actually, the transformation of **2** is very fast at the beginning and then slows down, a feature that might make one miss the true evolution. The first and the second CV recordings are only separated by ten minutes. For the next 8 h the POM continues to evolve slowly. This transformation is essentially reflected in the shape of the CV and not in a change in the current intensity. The difference between the voltammograms is more pronounced at lower pH. It is apparent that the transformation pathways are more intricate for **2** than for **1**. The intermixing of the CVs suggests the breakdown of **2** into mixtures of unidentified products. Comparison of Figure 3C and 3D confirms that **2** and [*A*-α-$AsW_9O_{34}]^{9-}$ do not reach the same final state. The two-wave final evolution CV of [*A*-α-$AsW_9O_{34}]^{9-}$ is analogous to the pattern obtained for the transformation of [*A*-α-$PW_9O_{34}]^{9-}$, with the potential location of the former being slightly more positive, as expected (vide supra).

These observations clearly indicate a stability difference between **1** and **2**. This difference is even more striking when the pH was lowered, while keeping the acetate medium. Therefore, we decided to study the pH dependence in detail. In addition, **1** was found to evolve slowly in a pH 3 acetate medium, which led us to also study the effects of the solution composition as well.

Influence of the pH and the solution composition: This study was performed by CV and the results confirmed a striking dependence on the solvent. We changed the solvent composition systematically in order to highlight these effects. The common reference point was the pH 3 CH_3COOLi medium, which exhibited the shortest stabilization time. Relying on the CV evolution in each solution, the following stability sequence was found for **1**: taking an arbitrary duration 1 for (1 M CH_3CO_2Li/CH_2ClCO_2H, pH 3), the duration is roughly 12 for (0.5 M Li_2SO_4/H_2SO_4, pH 3) and 33 for (1 M LiCl/HCl, pH 3). Evidently, sulfate ions have an appreciable stabilization effect, but the strongest effect, by far, is obtained with chloride ions. A complementary experiment with 1 M LiCl + 0.1 M CH_3CO_2Li + CH_2ClCO_2H (pH 3) gives a relative stability duration of only 3.9, thus supporting the above solvent-composition effect. In summary, the sequence of stabilization for **1** is: $Cl^- > SO_4^{2-} > CH_3COO^-$. Interestingly, **1** remains stable for a significantly longer time than **2**, in the same experimental conditions. The reasons for these observations are not yet clear.

The influence of electrolyte composition and of its ionic strength has been reported frequently in the polyoxometalate (POM) literature.[25,31–34] As far as anions in these mix-

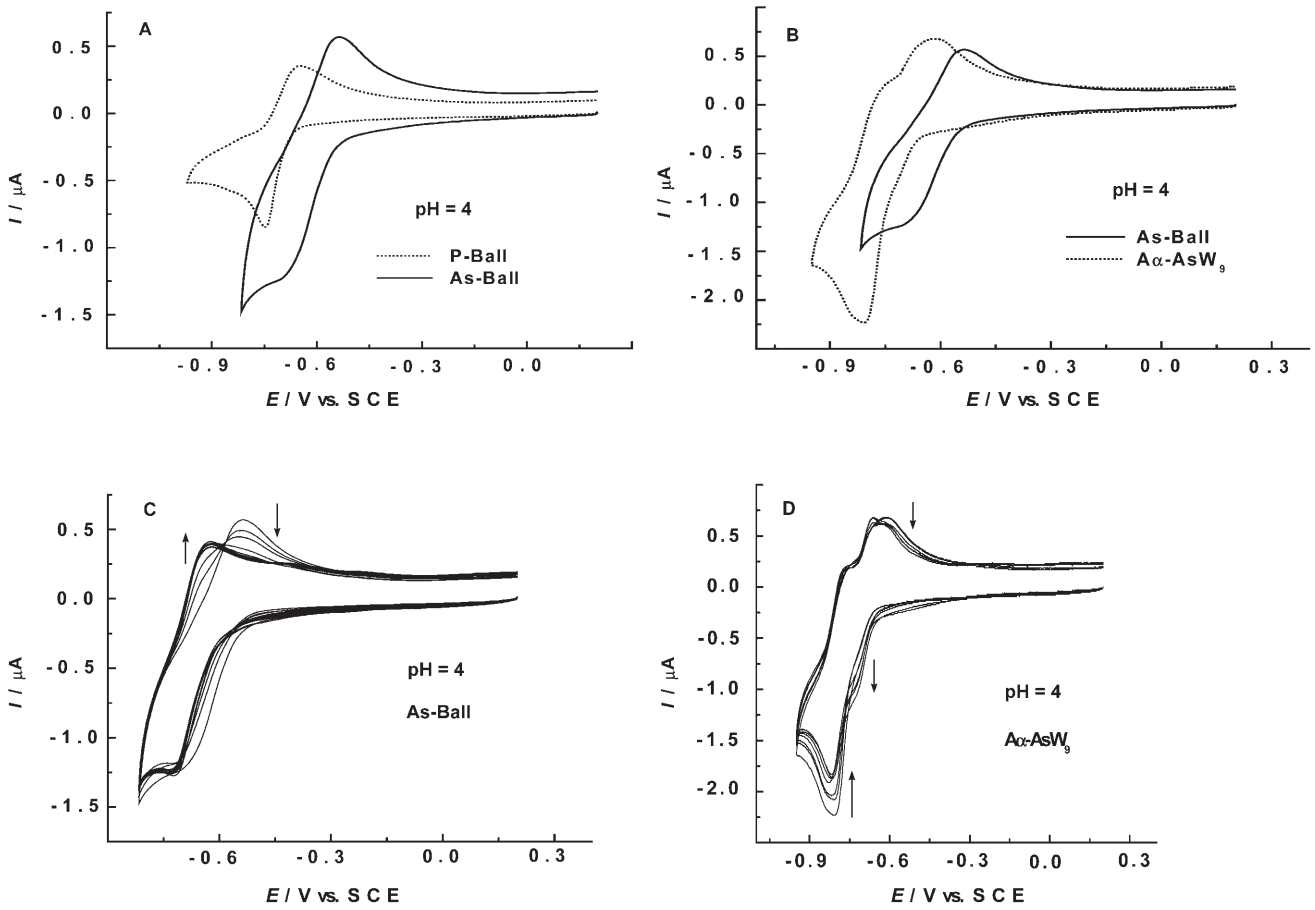

Figure 3. CVs of 2×10^{-5} M **1** and **2** in a pH 4 medium (1 M CH_3CO_2Li/CH_3CO_2H). The scan rate was 10 mV s^{-1}, the working electrode was glassy carbon and the reference electrode was SCE. A) Superposition of the "initial" CVs of **1** and **2**. B) Superposition of the "initial" CVs of **2** and 2×10^{-4} M [*A*-α-$AsW_9O_{34}]^{9-}$. C) Evolution of the CV of **2** with time. D) Evolution of the CV of 2×10^{-4} M [*A*-α-$AsW_9O_{34}]^{9-}$.

tures are concerned, it was shown recently that chloride ions can be associated with POM complexes[32,33] and even stabilize Fe^{II} centers.[34] The interaction of anions with POMs is an important and long-pending issue. By now this is a well-established fact, although it might at first sight appear to be counter-intuitive considering the overall negative charge of POMs. For instance, the coordination of nitrate to $\{Cu_3[A\text{-}\alpha\text{-}PW_9O_{34}]_2\}^{12-}$ was unambiguously demonstrated by IR spectroscopy and X-ray structure determination by Knoth et al.[31] According to these authors, "This complexation of an anion by an anion can be rationalized by postulating that there is little negative charge density in the region of the belt. The negative charge probably remains largely localized on the phosphate groups, whereas the belt, consisting of three dipositive metals, probably has positive charge." Also, IR spectra show the Co and Mn complexes to behave in the same way, but only the Mn complex retains nitrate upon recrystallization. "Nitrite also forms complexes with $\{Cu_3[A\text{-}\alpha\text{-}PW_9O_{34}]_2\}^{12-}$ and $\{Co_3[A\text{-}\alpha\text{-}PW_9O_{34}]_2\}^{12-}$." The observations made in the present experiments could be interpreted within the same framework. Firstly, we observed that only some anions interact favorably with **1**. For example, acetate and sulfate were not as effective as chloride in stabilizing **1**. Secondly, it is well established that the negative charge density on POMs is usually rather small and in fact similar to that of the perchlorate ion.[35] Thirdly, in close similarity with the example described by Knoth et al.,[31] **1** is composed of 12 trilacunary Keggin units pinned into position by 12 inner, cationic $(CH_3)_2Sn^{2+}$ groups and 24 outer, cationic $(CH_3)_2(H_2O)Sn^{2+}$ groups. The solid-state structure of **1** indicates that there are regions of localized positive charges on the spherical supercluster.

*Detailed electrochemical study of **1** in LiCl medium at pH 3*: The lithium chloride pH 3 medium was selected for a detailed electrochemistry study of **1** and **2**. In the case of **2**, CV studies revealed that it evolved right from the beginning of the experiments, and it was not possible to obtain two reproducible voltammograms. Actually, the changes were so rapid that it was not even possible to detect the very first cyclic voltammogram (see Figure 3).

The presence of lithium ions in the solvent medium rendered $\mathbf{Cs_{14}}$**-1** more soluble and relatively stable, particularly in 2 M LiCl, pH 3, as revealed by CV and spectrophotometry.

Successive scans had the same shape and peak potential locations, but the peak currents kept increasing with time, indicating an incomplete dissolution process of a fairly stable species. Such evolution is easily distinguished from a decomposition process, which is accompanied by wave splitting and potential change. In Figure 4A the progressive dissolution of **Cs_{14}-1** in 1 M LiCl, pH 3 medium is shown. Eventually, the curves became reproducible, about 2–3 h after the solution was prepared. Following complete dissolution, **1** remains stable in solution and only negligible evolution could be detected by CV after 9 h. This observation indicates the existence of a comfortable time window for a detailed electrochemistry characterization of **1**. The single wave shown in Figure 4A is followed at a more negative potential by a large current intensity wave close to the electrolyte discharge limit. This wave was not studied further. However, it is worth noting that **2** is completely unstable in this medium.

After the stabilization period, Figure 4B shows the peak current variations as a function of the potential scan rate and it can be seen that well-behaved voltammograms are obtained. The variation of the peak current intensity as a function of the square root of the scan rate is shown in Figure 4C. The very good linearity of this curve indicates that the voltammograms in Figure 4B feature a diffusion-controlled process. For comparison, Figure 4D shows the evolution of the CV of **2** in the same pH 3 medium, which kept evolving. Controlled potential coulometry for **1** indicates the consumption of roughly 25 electrons per polyanion in this pH 3 medium. Interestingly, the consumed electrons could be fully recovered upon reoxidation. However, the exact number of electrons cannot be determined reliably enough to estimate the diffusion coefficient of **1**.

An approximate value of the diffusion coefficient was obtained in the following manner. Polyanion **1** may be considered as an oligomer of $[A\text{-}\alpha\text{-}PW_9O_{34}]^{9-}$. In this case the diffusion coefficient of **1** (which is composed of 12 identical Keggin units) can be estimated, provided that the diffusion coefficient D_m of the monomer is known [Eq. (1)]:[36–38]

$$D = D_m(M_m/M_p)^{0.55} \quad (1)$$

In Equation (1) M_m and M_p are the molecular weights of $[A\alpha\text{-}PW_9O_{34}]^{9-}$ and **1**, respectively. For this purpose, it was assumed that the diffusion coefficient of $[PW_{12}O_{40}]^{3-}$ is a good estimate for that of $[A\text{-}\alpha\text{-}PW_9O_{34}]^{9-}$ and so the value of $D_m = 4.25\times10^{-6}\,cm^2s^{-1}$ was selected.[1,39,40] A crude esti-

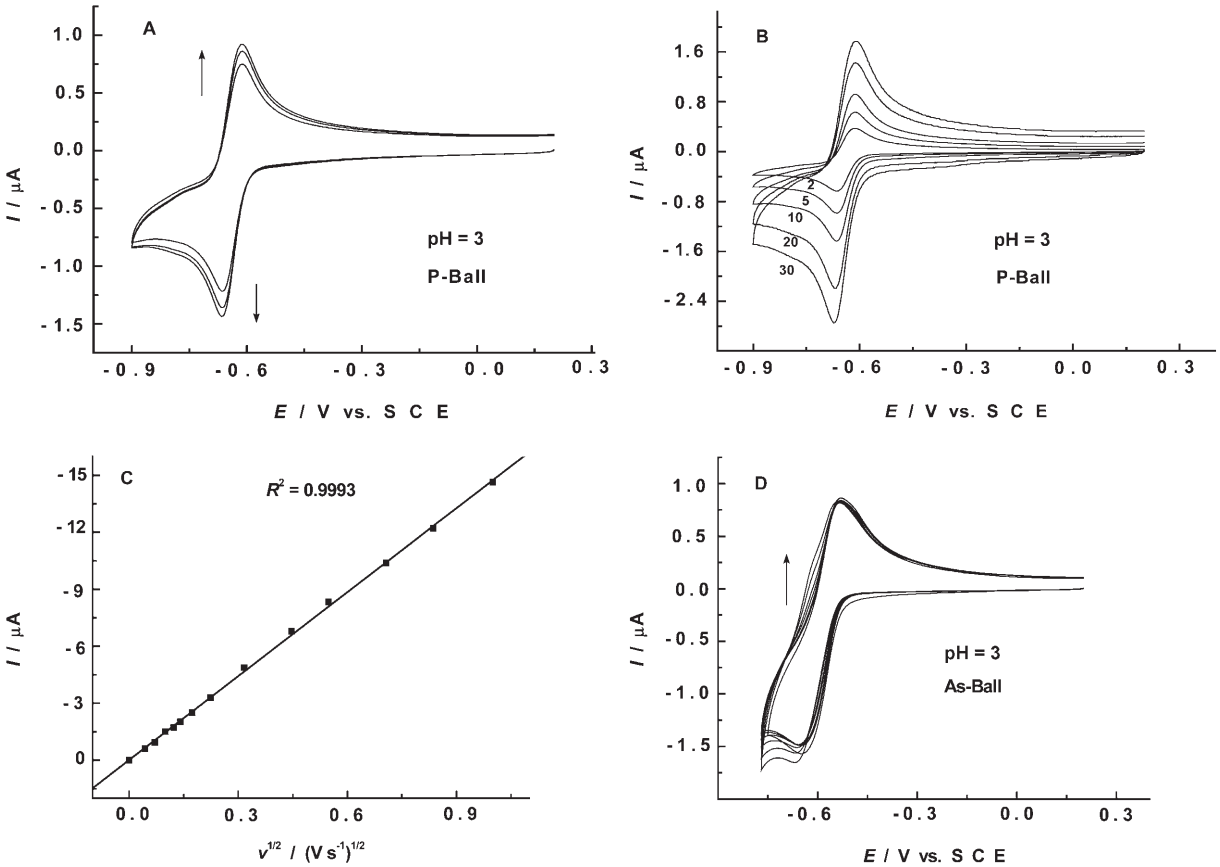

Figure 4. CVs and peak current intensity variations for 2×10^{-5} M **1** and **2** in a pH 3 medium (1 M LiCl/HCl). The working electrode was glassy carbon and the reference electrode was SCE. A) CVs reflecting the continuous dissolution of **1**. The scan rate was 10 mV s^{-1}. B) CVs of completely dissolved **1** as a function of scan rate. The scan rate values appear on each curve in mV s^{-1}. C) Variations of peak current intensities as a function of the square root of scan rate. D) Evolution of the CV of **2** as a function of time in the pH 3 medium. The scan rate was 10 mV s^{-1}.

mate of the diffusion coefficient for **1** would then be $D = 9.7 \times 10^{-7}\,cm^2 s^{-1}$. By using this value in conjunction with the Stokes–Einstein equation, a radius $r = 2.2$ nm could be estimated for **1**. This value is slightly larger than the 1.5 nm from crystallographic data,[19] but when including the water molecules of hydration around **1** in solution and taking into account the approximate choice of $[A\text{-}\alpha\text{-}PW_9O_{34}]^{9-}$ as the appropriate monomer, it appears to be a quite good estimate.

Taking advantage of the stability of **1** in various media in the timescale of the present investigations, the formal potentials (E^0, calculated as the average between the cathodic and anodic peak potentials) were determined as a function of the pH and then compared. In acetate media, $\Delta E^0 = 91$ mV was determined for pH 3–4; in LiCl media, $\Delta E^0 = 86$ mV was found for pH 2–3.1. Roughly, a variation of 90 mV per pH unit can be identified.

The anodic to cathodic peak potential differences, ΔE_p, undergo two distinct variation regimes as a function of the potential scan rate. From $v = 2$ to roughly 30 $mV s^{-1}$, ΔE_p remains practically constant, ranging from 50 to 59 mV. For larger values of v, ΔE_p increases with the scan rate. In a chloride medium pH 3, ΔE_p reaches 68 mV at 50 $mV s^{-1}$ and 280 mV at 1 $V s^{-1}$. Such variations might suggest an overall quasi-reversible electron-transfer process. Such relatively simple behavior is expected for multiple electron transfers to a molecule containing any number of identical, non-interacting redox centers.[38] This observation supports the assumption to consider **1** as an oligomer of $[A\text{-}\alpha\text{-}PW_9O_{34}]^{9-}$. However, this conclusion should be considered with caution, due to the important participation of protons in the reaction pathway. Figure 5 compares the CVs observed for **1**, after stabilization, in LiCl media at pH 2, 3, and 4, and highlights this proton participation. The wave at pH 2 is well-behaved, but slightly composite, with a large peak current intensity and a ΔE_p value corresponding to a relatively fast electron-transfer process. Upon increasing the pH, the current decreases and the whole CV is shifted in the negative potential direction accompanied by an increase in ΔE_p values. A relatively low ionic strength is probably not the reason for this observation. An analogous behavior was previously observed when a large concentration of Li^+ ions did not compensate for the lack of buffer capacity of the medium.[25,26] The behavior also underscores the essential role of protons in the electrochemistry of POMs.

Solid-state electrochemistry of 1 immobilized in a carbon-paste electrode: To complement the solution studies on **1** (vide supra) we also decided to investigate this POM in the solid state by entrapping $\mathbf{Cs_{14}}$**-1** in a carbon paste. The advantages of using carbon-paste electrodes (CPEs) in electroanalysis and in electrocatalysis, in particular upon their bulk modification by metal particles or by enzymes, have been discussed in several papers.[24,41–46] In the present case, the build-up of a solid-state assembly is favored by the well-known strong adhesion of POMs to the graphite substrate.[47] As a consequence, the solid-state study discussed here is different from the direct electrochemistry on a POM single crystal as described in the literature.[48] In fact, it should rather be paralleled with the entrapment of POMs within polymer matrices resulting in the build-up of insoluble assemblies.[49] Such assembly is so tight that no leaking of the CPE electrode is expected.[47,49]

Based on the results illustrated in Figure 5, we decided to investigate first such immobilized **1** by CV in a 1 M LiCl/HCl pH 2 medium. The potential scan rate was varied between 10 and 200 $mV s^{-1}$. The potential domain explored in Figure 5 was kept for the present experiments. Figure 6 (full line curve) shows a representative CV obtained with the carbon-paste electrode, in the pH 2 electrolyte, at a potential scan rate of 100 $mV s^{-1}$. For direct comparison, the corresponding CV with **1** in solution was run at the same scan rate. At least two types of remarkable observations deserve attention. Firstly, a single multi-electron wave is obtained both in the solid state and in solution. This pattern is reproducible as a function of time. This behavior must be contrasted with the two-step CV pattern associated with the de-

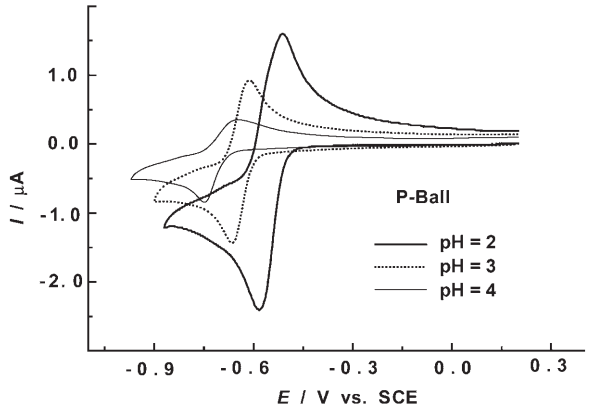

Figure 5. CVs of solutions with completely dissolved **1** (2×10^{-5} M) in pH 2, 3, and 4 media (1 M LiCl/HCl). The scan rate was 10 $mV s^{-1}$, the working electrode was glassy carbon and the reference electrode was SCE.

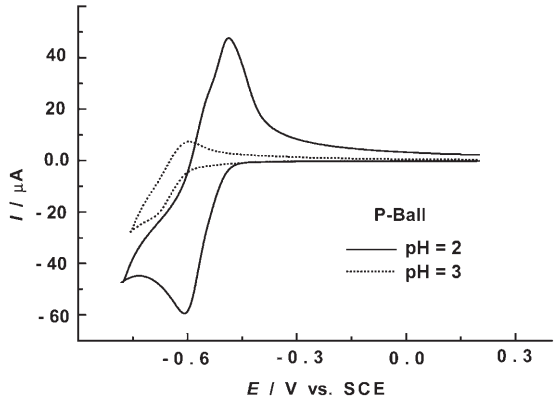

Figure 6. CVs of $\mathbf{Cs_{14}}$**–1** immobilized in a carbon-paste electrode, run in pH 2 and 3 media (1 M LiCl/HCl). The scan rate was 100 $mV s^{-1}$ and the reference electrode was SCE.

composition of **1** in the absence of chloride ions (e.g., see Figures 2A and 2D). These characteristics point to the stability of **1** in the carbon paste. Secondly, the well-behaved, but slightly composite shape observed for the wave of **1** in solution is identical to the wave obtained with the polyanion entrapped in the carbon paste. By and large, it is expected that the organic matrix should decrease the rates of electron transfer and thus create substantial overvoltages for certain analytes.[43] Indeed, such a trend appears in the anodic-to-cathodic peak potential difference in Figure 6 as compared to the same parameter in Figure 4B. However, it is worth noting that only a negligible difference exists between the reduction peak potential locations of the waves obtained for **1** in the carbon paste and in solution. Altogether, these observations support the conclusions that identical polyanion structures exist in the carbon paste and in the 1 M LiCl/HCl pH 2 solution and this species is believed to be **1**. Finally, Figure 6 shows the CVs obtained with the carbon-paste electrode loaded with **1** in chloride media at pH 2 (full line curve) and pH 3 (dotted line curve). As already observed previously (see Figure 4), when the pH increases the current decreases and the entire CV is shifted in the negative potential direction. Even though the POM is not diffusing freely in solution and reacts mainly in the interfacial region, this feature underscores once again the important role of protons in the electrochemistry of POMs.

Work is in progress towards the optimization of the present immobilization procedure and its comparison with other immobilization techniques, with the ultimate goal to use such assemblies for catalytic processes.

Electrocatalytic behavior of 1 towards NO_x: The electrocatalytic reduction of nitrate ions is one of the challenging problems in the NO_x series, because a complete process requires several electrons. Above we have demonstrated that **1** may be considered as a multi-electron reservoir and as a result, it is a very promising candidate for an efficient reduction of nitrate. Therefore, we decided to investigate the electrocatalytic activity of **1** as concerns the reduction of nitrate. Considering that nitrite and nitric oxide are likely intermediates in the reduction of nitrate, we also performed a complementary study with these substrates.

Electrocatalytic reduction of nitrate and nitrite: The first cyclic voltammetric wave of **1** in a pH 2 medium and in the absence and presence of nitrate is shown superposed in Figure 7A. We have checked that the direct reduction of nitrate does not occur in the potential domain explored in Figure 7A. The chemically reversible single wave of **1** becomes irreversible in the presence of nitrate at pH 2; its cathodic peak current increases substantially and splits into two large current waves. It should be noted that the first of these catalytic waves is polarogram-shaped, and eventually the second wave shows a similar tendency. At least two observations deserve attention. Firstly, the W-wave of **1** showing catalytic behavior is located at −0.585 V versus SCE, a remarkably positive potential compared to the catalytic waves of related

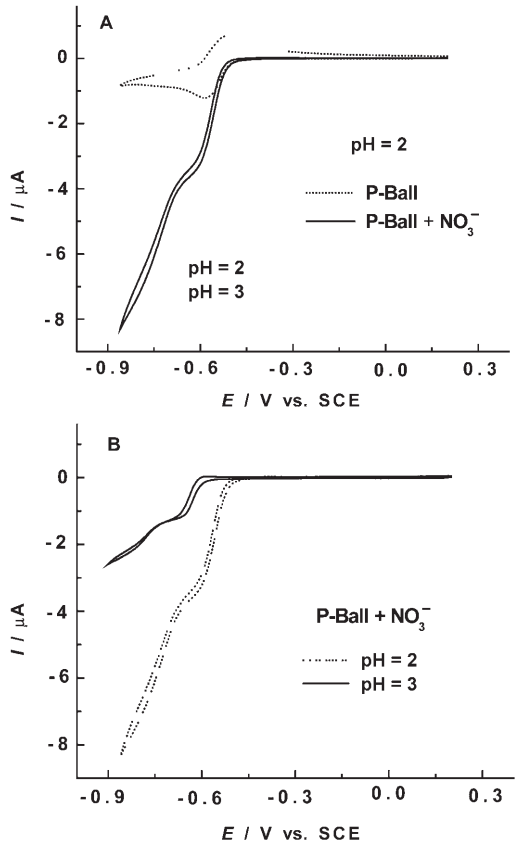

Figure 7. CVs of 2×10^{-5} M **1** in pH 2 or pH 3 medium (1 M LiCl/HCl) in the presence of nitrate. The scan rate was 2 mV s^{-1}; the working electrode was glassy carbon and the reference electrode a saturated calomel electrode. A) CVs of **1** in pH 2 medium (1 M LiCl/HCl) addressing just the first redox processes of the W centers, in the absence and presence (1 M) of nitrate. B) Comparison of the CVs of **1** + 1 M nitrate at pH 2 and pH 3, respectively.

POM systems. Secondly, the accumulation of a very large number of electrons at this wave is a truly remarkable feature. These characteristics allow **1** to be included in the very small class of POMs that are capable of electrocatalytically reducing nitrate. As a matter of fact, the POM size is not a sufficient prerequisite, as for example the cyclic tungstophosphate $[H_7P_8W_{48}O_{148}]^{33-}$ fails to catalyze the reduction of nitrate even at the potential of its 16-electron wave.[25] The catalytic efficiency of **1** might be attributed to a beneficial effect of the dimethyltin linkers. To date, only copper-, nickel-, and iron-containing POMs proved efficient for nitrate reduction.[50–55] Figure 7B shows the pH dependence of nitrate reduction by **1** and qualitatively we observe the same behavior at pH 2 and 3. The catalytic pattern moves in the negative potential direction with increasing pH, in complete agreement with the behavior of **1** in the absence of nitrate (see Figure 5). Interestingly, nitrite is reduced by **1** at a potential that is around 150 mV more positive compared to nitrate reduction. Therefore we conclude that **1** reduces nitrate beyond the state of nitrite. In addition, previous work from this group[56] has demonstrated the quantitative conversion of NO into N_2O by a selection of one- and two-elec-

tron-reduced POMs. In the present case, accumulation of electrons in the POM framework as observed with **1** is, thus, likely to produce highly reduced nitrogen compounds.[25,57]

*Interaction of **1** with NO—a perspective view for biological and biomimetic applications*: Several large POMs such as $[H_7P_8W_{48}O_{148}]^{33-}$[25] and $[Co(H_2O)_2\{(SiW_9O_{34})(SiW_8O_{31})Co_3(H_2O)\}_2]^{26-}$[58] have been shown to be effective electrocatalysts for redox reactions involving NO_x species in general and NO in particular. The interest in NO has grown considerably ever since its important role in biology was unveiled. It seems that NO is not just a pollutant when released in the atmosphere, but it rather works as a molecular messenger and is implicated in oxidative stress response as well. Therefore we decided to study **1** (the more stable of the two ball-shaped POMs used in this work) by CV in the presence of NO. We discovered a sharp increase in the reduction current, which keeps increasing with time (Figure 8A). One might attribute this behavior to NO alone, but two observations rule out this possibility: 1) the onset of the reduction wave of **1** is 60 mV more positive in the presence of NO, perhaps suggesting an association between **1** and NO resulting in an assembly which is more easily reduced than **1** alone; and 2) the reduction potential of free NO ($E_c = -0.890$ V) is more negative than that of free **1** ($E_c = -0.630$ V), see Figure 8B. A similar behavior was observed for plenary POMs such as Wells–Dawson ($[P_2W_{18}O_{62}]^{6-}$) and Keggin ($[SiW_{12}O_{40}]^{4-}$) species. However, in these cases the current increase was not as pronounced and there was no noticeable activation of the NO reduction. Also in the present example, a voltammogram virtually identical to the original one is found after bubbling argon through the solution. Nevertheless, complete removal of NO by this procedure was difficult. It seems that a labile interaction exists between **1** and NO, so that the two species separate when the concentration of NO is considerably decreased. Close inspection of the structure of **1** (see Figure 1) suggests that NO might replace some of the terminal, labile water molecules attached to the 24 outer dimethyltin groups. Alternatively, it is possible that NO enters the large, hydrophobic, central pocket of **1** by passing through its surface pockets. This appears to be possible in solution for small guest molecules like NO. The real nature of this perfectly reproducible interaction is not yet understood. More work is needed to pin down the actual mechanism of this phenomenon.

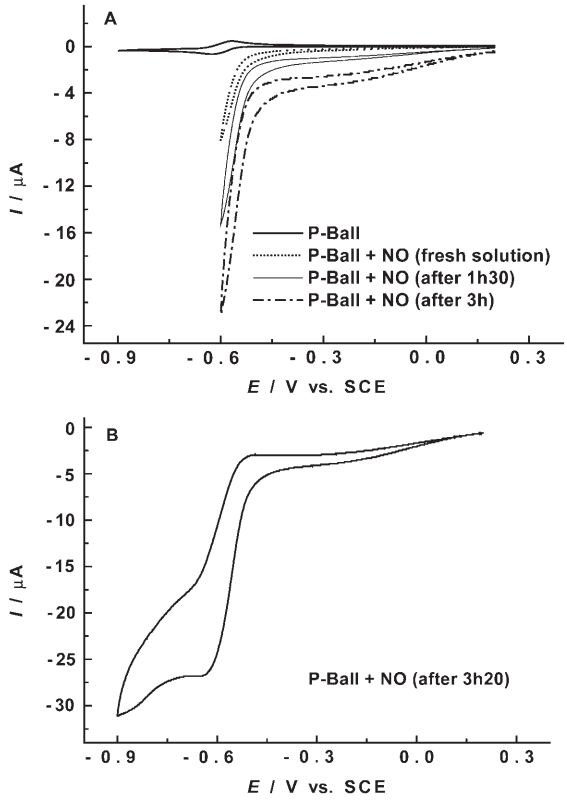

Figure 8. CVs of 2×10^{-5} M **1** in pH 3 medium (1 M LiCl/HCl) in the presence of NO. The scan rate was 2 mV s^{-1}; the working electrode was glassy carbon and the reference electrode a saturated calomel electrode. A) CVs of **1** addressing just the first redox processes of the W centers, without NO and at several time intervals after saturation with NO ([NO] = 1 to 2 mM). B) CV of **1** + NO showing the final catalytic reduction peak 3 h 20 min after NO saturation.

Conclusions

The two polyanions **1** and **2** were studied with the aim to detect a time window during which their stability will allow a comfortable electrochemical characterization of their redox and electrocatalytic behaviors.

Polyanions **1** and **2** and their corresponding salts **Cs_{14}-1** and **Cs_{14}-2** exhibit quite different solubility and stability characteristics in various aqueous electrolytes. **Cs_{14}-2** is readily soluble to concentration levels useful for electrochemical studies, whereas the low solubility of **Cs_{14}-1** limited the study to concentrations of 2×10^{-5} M. Furthermore, the dissolution of **Cs_{14}-1** is favored by the presence of Li^+ ions in solution, but still remains a slow process. An important stabilization is observed in chloride-containing media. Gel filtration rules out an eventual decay of either **1** or **2** down to monomeric derivatives, with molecular masses between 2000 and 3000 g mol^{-1} on the timescale of the experiment. However, UV/Vis spectroscopy and cyclic voltammetry reveal that **2** is significantly less stable than **1**. The two POMs also show different decomposition patterns, while their respective lacunary precursors $[A\text{-}XW_9O_{34}]^{9-}$ (X = P, As) follow parallel transformation pathways. The transformations of **1** are similar to those of $[A\text{-}PW_9O_{34}]^{9-}$, whereas **2** and $[A\text{-}AsW_9O_{34}]^{9-}$ seem to follow different transformation pathways. Polyanion **1** first collapses into monomeric derivatives which might contain $[A\text{-}PW_9O_{34}]^{9-}$. The final monomeric decomposition products of **1** appear to contain $[PW_{11}O_{39}]^{7-}$ or $[A\text{-}PW_9O_{34}]^{9-}$ with dimethyltin fragments attached (e.g., $[\{Sn(CH_3)_2(H_2O)_2\}_xPW_9O_{34}]^{(9-2x)-}$, x = 1–3). The fairly long-term stability of **1** in 1 M LiCl, pH 3 medium allowed for its electrochemical study. The main observation here is that the self-assembly of 12 $[A\text{-}PW_9O_{34}]^{9-}$ units

through 36 $\{Sn(CH_3)_2\}^{2+}$ groups into the 3 nm ball-shaped, empty **1** results in a new and remarkable behavior. The pH domain in which **1** is fairly stable is larger than that observed for
$[A\text{-}PW_9O_{34}]^{9-}$. In the pH 4 medium in which both polyanions could be studied, the smaller value of the anodic-to-cathodic peak potential difference ΔE_p for **1** indicates faster overall electron-transfer kinetics compared to the trilacunary precursor. Solid-state electrochemistry of $\mathbf{Cs_{14}}$-**1** entrapped in a carbon-paste provides complementary support for the conclusion that **1** is stable in appropriate chloride-containing media over the timescale of several hours. This observation might open new perspectives for studying the properties of such molecules.

To our knowledge, **1** constitutes the first example of a molecule that can uptake such a large number of electrons reversibly at a single potential. These properties show promise for future fundamental and applied studies. A key requirement is to discover media suitable for higher solubility and stabilization of these potentially important electron reservoirs. The dodecameric **1** is a new example of a POM that exhibits efficient electrocatalytic reduction of nitrate, which, in fact, is being reduced beyond the state of nitrite.

The remarkable interaction of **1** with NO might open ways to investigate the biomimetic properties of this POM.

In future work we also plan to explore the medicinal properties of **1** and **2** in a biocompatible environment. In particular, we would like to explore the central, hydrophobic cavities of **1** and **2**, which could, in theory, be loaded with hydrophobic drugs. It is planned to investigate the effects of **1** and **2** on Hela cancer cells both in solution and also supported on poly-L-lysine films. Indeed, deliberate entrapment of pharmaceutically active compounds in thin films or oligomeric containers with the aim to fabricate sustained-release coatings has recently become an area of intense research activity.

Acknowledgements

This work was supported by the CNRS (UMR 8000) and the Université Paris-Sud 11 and the Jacobs University of Bremen (JUB). We thank Dr. Santiago Reinoso (JUB) for the preparation of $\mathbf{Cs_{14}}$-**1 and** $\mathbf{Cs_{14}}$-**2**.

[1] M. T. Pope in *Heteropoly and Isopoly Oxometalates*, Springer, Berlin, **1983**.
[2] M. T. Pope, A. Müller, *Angew. Chem.* **1991**, *103*, 56–70; *Angew. Chem. Int. Ed. Engl.* **1991**, *30*, 34–48.
[3] *Polyoxometalates: from Platonic Solids to Anti-Retroviral Activity* (Eds.: M. T. Pope, A. Müller), Kluwer, Dordrecht (The Netherlands), **1994**.
[4] "Polyoxometalates": *Chem. Rev.* **1998**, *98*, 1–389.
[5] *Polyoxometalate Chemistry: From Topology via Self-Assembly to Applications* (Eds.: M. T. Pope, A. Müller), Kluwer, Dordrecht (The Netherlands), **2001**.
[6] C. L. Hill in *Comprehensive Coordination Chemistry II: Transition Metals Groups 3–6* (Ed.: A. G. Wedd) Elsevier Science, New York, **2004**, pp. 679–759.
[7] "Electrochemistry of Isopoly and Heteropoly Oxometalates": B. Keita, L. Nadjo, *Encycl. Electrochem.* **2006**, *7*, 607–700.
[8] B. Krebs, I. Paulat-Böschen, *Acta Crystallogr. Sect. B* **1982**, *38* 1710–1718.
[9] M. Leyrie, G. Hervé, *Nouv. J. Chim.* **1978**, *2*, 233–237.
[10] R. Contant, A. Tézé, *Inorg. Chem.* **1985**, *24*, 4610–4614.
[11] R. Contant, *Inorg. Synth.* **1990**, *27*, 104–111.
[12] A. Müller, B. Botar, S. K. Das, H. Bögge, M. Schmidtmann, A. Merca, *Polyhedron* **2004**, *23*, 2381–2385.
[13] A. Müller, S. Q. N. Shah, H. Bögge, M. Schmidtmann, *Nature* **1999**, *397*, 48–50.
[14] K. Wassermann, M. H. Dickman, M. T. Pope, *Angew. Chem.* **1997**, *109*, 1513–1516; *Angew. Chem. Int. Ed. Engl.* **1997**, *36*, 1445–1448.
[15] E. Cadot, M. A. Pilette, J. Marrot, F. Sécheresse, *Angew. Chem.* **2003**, *115*, 2223–2226; *Angew. Chem. Int. Ed.* **2003**, *42*, 2173–2176.
[16] U. Kortz, M. G. Savelieff, B. S. Bassil, M. H. Dickman, *Angew. Chem.* **2001**, *113*, 3488–3491; *Angew. Chem. Int. Ed.* **2001**, *40*, 3384–3386.
[17] F. Hussain, B. S. Bassil, L-H. Bi, M. Reicke, U. Kortz, *Angew. Chem.* **2004**, *116*, 3567–3571; *Angew. Chem. Int. Ed.* **2004**, *43*, 3485–3488.
[18] U. Kortz, S. S. Hamzeh, N. A. Nasser, *Chem. Eur. J.* **2003**, *9*, 2945–2952.
[19] U. Kortz, F. Hussain, M. Reicke, *Angew. Chem.* **2005**, *117*, 3839–3843; *Angew. Chem. Int. Ed.* **2005**, *44*, 3773–3777.
[20] P. J. Domaille, *Inorg. Synth.* **1990**, *27*, 100–104.
[21] R. Contant, *Can. J. Chem.* **1987**, *65*, 568–573.
[22] R. Contant, R. Thouvenot, *Can. J. Chem.* **1991**, *69*, 1498–1506.
[23] B. Keita, L. Nadjo J. , *Electroanal. Chem.* **1988**, *243*, 87–103.
[24] H. Remita, P. F. Siril, I. M. Mbomekalle, B. Keita, L. Nadjo, *J. Solid State Electrochem.* **2006**, *10*, 506–511.
[25] B. Keita, Y. W. Lu, L. Nadjo, R. Contant, *Electrochem. Commun.* **2000**, *2*, 720–726.
[26] B. Keita, Y. W. Lu, L. Nadjo, R. Contant, *Eur. J. Inorg. Chem.* **2000**, 2463–2471.
[27] B. S. Bassil, U. Kortz, A. S. Tigan, J. M. Clemente-Juan, B. Keita, P. de Oliveira, L. Nadjo, *Inorg. Chem.* **2005**, *44*, 9360–9368.
[28] G. C. Chorghade, M. T. Pope, *J. Am. Chem. Soc.* **1987**, *109*, 5134–5138.
[29] F. Hussain, U. Kortz, B. Keita, L. Nadjo, M. T. Pope, *Inorg. Chem.* **2006**, *45*, 761–766.
[30] R. Contant, G. Hervé, *Rev. Inorg. Chem.* **2002**, *22*, 63–111.
[31] W. H. Knoth, P. J. Domaille, R. L. Harlow, *Inorg. Chem.* **1986**, *25*, 1577–1584.
[32] W. J. Randall, T. J. R. Weakley, R. G. Finke, *Inorg. Chem.* **1993**, *32*, 1068–1071.
[33] T. M. Anderson, X. Zhang, K. I. Hardcastle, C. L. Hill, *Inorg. Chem.* **2002**, *41*, 2477–2488.
[34] B. Keita, I. M. Mbomekalle, L. Nadjo, T. M. Anderson, C. L. Hill, *Inorg. Chem.* **2004**, *43*, 3257–3263.
[35] L. Barcza, M. T. Pope, *J. Phys. Chem.* **1975**, *79*, 92–93.
[36] F. G. Bordwell, G. D. Cooper, H. Morita, *J. Am. Chem. Soc.* **1957**, *79*, 376–378.
[37] T. W. Smith, J. E. Kuder, D. Wychick, *J. Polym. Sci. Polym. Chem. Ed.* **1976**, *14*, 2433–2448.
[38] J. B. Flanagan, S. Margel, A. J. Bard, F. C. Anson, *J. Am. Chem. Soc.* **1978**, *100*, 4248–4253.
[39] B. Keita, T. Lucas, L. Nadjo, *J. Electroanal. Chem. Interfacial Electrochem.* **1986**, *208*, 343–356.
[40] L. C. W. Baker, M. T. Pope, *J. Am. Chem. Soc.* **1960**, *82*, 4176–4179.
[41] R. N. Adams, *Anal. Chem.* **1958**, *30*, 1576–1578.
[42] L. S. Marcoux, K. B. Prater, B. G. Prater, R. N. Adams, *Anal. Chem.* **1965**, *37*, 1446–1447.
[43] M. E. Rice, Z. Galus, R. N. Adams, *J. Electroanal. Chem. Interfacial Electrochem.* **1983**, *143*, 89–102.
[44] J. Wang, N. Naser, L. Angnes, H. Wu, L. Chen, *Anal. Chem.* **1992**, *64*, 1285–1288.
[45] K.-H. Lubert, M. Guttmann, L. Beyer, *J. Electroanal. Chem.* **1999**, *642*, 174–180.

[46] G-Y. Kim, N. M. Cuong, S-H. Cho, J. Shim, J-J. Woo, S-H. Moon, Talanta **2007**, *7*, 129–135.
[47] Y. Izumi, K. Urabe, *Chem. Lett.* **1981**, 663–666.
[48] P. J. Kulesza, L. R. Faulkner, *J. Am. Chem. Soc.* **1993**, *115*, 11878–11884.
[49] B. Keita, K. Essaadi, L. Nadjo, *J. Electroanal. Chem. Interfacial Electrochem.* **1989**, *259*, 127–146.
[50] D. Jabbour, B. Keita, L. Nadjo, U. Kortz, S. S. Mal, *Electrochem. Commun.* **2005**, *7*, 841–847.
[51] B. Keita, E. Abdeljalil, L. Nadjo, R. Contant, R. Belghiche, *Electrochem. Commun.* **2001**, *3*, 56–62.
[52] B. Keita, I. M. Mbomekalle, L. Nadjo, R. Contant, *Electrochem. Commun.* **2001**, *3*, 267–273.
[53] B. Keita, I. M. Mbomekalle, L. Nadjo, *Electrochem. Commun.* **2003**, *5*, 830–837.
[54] D. Jabbour, B. Keita, I. M. Mbomekalle, L. Nadjo, U. Kortz, *Eur. J. Inorg. Chem.* **2004**, 2036–2044.
[55] L-H. Bi, U. Kortz, S. Nellutla, A. C. Stowe, J. van Tol, N. S. Dalal, B. Keita, L. Nadjo, *Inorg. Chem.* **2005**, *44*, 896–903.
[56] A. Belhouari, B. Keita, L. Nadjo, R. Contant, *New J. Chem.* **1998**, *22*, 83–86.
[57] J. E. Toth, F. C. Anson, *J. Am. Chem. Soc.* **1989**, *111*, 2444–2451.
[58] L. Lisnard, P. Mialane, A. Dolbecq, J. Marrot, J. M. Clemente-Juan, E. Coronado, B. Keita, P. de Oliveira, L. Nadjo, F. Sécheresse, *Chem. Eur. J.* , **2007**, 13, 3525–3536.

Received: December 22, 2006
Published online: April 19, 2007

